A model for variation of velocity vs. density trends in porous sedimentary rocks

David C. DeMartini

Lone Star Geophysical Consulting, Houston, Texas 77024

Michael E. Glinsky

BHP Billiton Petroleum, Houston, Texas 77056

A rock physics model appropriate for porous media in which some of the solid material is "floating" or not involved in load support is developed that explains observed variation in compressional wave velocity vs. density trends. This same model predicts no significant change in the shear vs. compressional wave velocity trend, as is also observed. These floating grains are correlated with a lack of sorting of the matrix grains as expected. The presence of the floating grains is found to correlate with a decrease in the permeability of the rock and therefore the viability of potential petroleum reservoirs. Shifts in the velocity vs. density relationships can be determined by wireline log but not directly by seismic reflectivity measurements. However, the introduction of an additional concept, the capture fraction of smaller grains, adds another constraint to the model which enables remote sensing of the viability of certain petroleum reservoirs by seismic reflectivity measurements alone. Experimental evidence is described that supports this model and additional experiments are suggested to further confirm it.

43.20.El, 43.40.Ph, 62.30.+d, 91.65.-n

I. BACKGROUND

Seismic reflection amplitudes have now been used for 35 years in prospecting for oil and gas reserves in certain types of sedimentary rocks. For rocks with high porosities and low bulk moduli the substitution of more compressible fluids such as oil or gas for less compressible fluids such as brine results in a significant reduction in both the density and particularly the compressional wave propagation velocity. Consequently, this also impacts the acoustic impedance of such reservoir rocks, thus affecting the reflection coefficient at interfaces between them and the impermeable sealing rocks with which they are in contact. This phenomenon was described in detail in the low frequency limit by Gassmann[1] and subsequently dynamically by Biot[2] several decades ago. At common seismic prospecting frequencies of 10 - 100 Hz, the low frequency limit of Gassmann is an appropriate description for typical sedimentary rocks. For a macroscopically isotropic and homogeneous porous medium with a connected solid framework or matrix and a connected pore space in which a single pore fluid pressure can be defined, the applicable equations may be written in the form

$$\rho = \rho_g(1-\phi) + \rho_f\phi, \tag{1}$$

$$\rho V_p^2 = K_g\left[\frac{3(1-\nu_m)}{(1+\nu_m)}\beta + \frac{(1-\beta)^2}{\phi(\frac{K_g}{K_f}-1)+1-\beta}\right], \tag{2}$$

and

$$\rho V_s^2 = \mu_m = K_g\frac{3(1-2\nu_m)}{2(1+\nu_m)}\beta; \tag{3}$$

where ρ_g and K_g are the density and bulk modulus respectively of the solid or granular material of which the rock matrix is constructed, ρ_f and K_f are the corresponding properties of the pore fluid, ϕ is the porosity or fluid volume fraction of the rock, K_m, μ_m and ν_m are the bulk modulus, shear modulus and Poisson's ratio respectively of the evacuated porous rock matrix, $\beta = K_m / K_g$, and V_p and V_s are the compressional (P) and shear (S) wave propagation velocities in the fluid-saturated rock. If ρ, V_p and V_s are known along with the grain and fluid elastic properties for a particular pore fluid such as brine, these equations can be solved for values of the dimensionless quantities β and ν_m which do not depend on the pore fluid and then V_p and V_s can be calculated for a new pore fluid such as oil or gas using these values.

The critical determinant of the magnitude of the fluid substitution effect on the P-wave velocity is the $V_p(\phi)$ or equivalently, $V_p(\rho)$, relation for the normal brine-saturated rocks at a given location. Such relations are commonly determined from wireline log measurements of both ρ and the vertical V_p made in previous wells. Of course, such relations can and do vary spatially even in the same geologic province in which neither the mineralogy nor deposition mechanism might be expected to vary significantly. In this paper, we propose a model which may account for some of these differences and compare it with some recent field observations.

II. EXTENSION TO ROCK PHYSICS MODEL

Consider a porous rock in which a second dispersed solid component is introduced with elastic properties ρ_g^*, K_g^* and μ_g^* so that the porous rock remains

macroscopically homogeneous and isotropic. Suppose some fraction, f, of this second solid component consists of load bearing grains which are substituted in the rock matrix for grains composed of the first solid material whereas the rest of this second solid component exists in the pores but is not attached to the solid matrix of the rock and thus does not contribute to the matrix moduli but is instead suspended in the pore fluid. One may then use Eq. (1) to Eq. (3) to describe the density and velocities in the porous rock but with modified constituent properties. Let f^* be the volume fraction of the rock occupied by the second solid component. The volume fraction of this rock occupied by the first solid component is now $f_g = 1 - f^* - \phi$ and the volume fraction of the rock occupied by the suspended or floating fraction of the second solid material is $\phi_{flt} = (1-f) f^*$. The volume fraction of the rock which is not load bearing and, thus, not contributing to K_m or μ_m is then $\hat{\phi} = \phi + \phi_{flt}$ and $\hat{\phi}$, the structural or matrix porosity, must replace ϕ in Eq. (2). The density of the composite rock is then

$$\rho = f_g \rho_g + f^* \rho_g^* + \phi \rho_f = \rho_g + (\rho_g^* - \rho_g) f^* - (\rho_g - \rho_f)\phi . \tag{4}$$

Note that ρ is independent of f so if $\rho_g^* = \rho_g$, ρ does not change.

The bulk modulus of the suspension in the rock pore space is now given by the Reuss[3] bound since both components are subjected to the same pressure and so in this two component case K_f must be replaced by $\hat{K}_f$, where

$$\hat{K}_f = \frac{(\phi + \phi_{flt})}{(\phi + \frac{K_f}{K^*}\phi_{flt})} K_f . \tag{5}$$

The bulk modulus of the composite solid material in the rock matrix, $\hat{K}_g$,which must replace K_g in Eqs. (2) and (3), may be estimated by the arithmetic average of their Reuss and Voight[4] bounding bulk moduli as suggested by Hill[5].

It remains only to estimate the matrix moduli for this rock. At high differential pressures these matrix moduli will be functions only of the details of the microscopic geometry of the rock matrix. Since a representative value cannot be calculated even when a rock sample is available, one must use a reasonable functional form dependent on only macroscopic matrix geometry variables the principal one of which is $\hat{\phi}$. An empirical but useful approximation for $\beta = K_m / \hat{K}_g$ is

$$\beta = (1 - \frac{\hat{\phi}}{\hat{\phi}_0})^{\lambda} . \qquad (6)$$

This form has the useful properties that $\beta = 1$ as it must at $\hat{\phi} = 0$ and $\beta = 0$ at $\phi_0 = \hat{\phi}_0$ which it must at the suspension limit where there is no load-bearing matrix. $\hat{\phi}_0$ and λ may be estimated by fitting values of β derived from measured wireline log data where $\phi_{flt} = 0$. For averages of data from a large number of locations in the petroleum province under study, sediments with consistent $V_p(\rho)$ trends, we find $\hat{\phi}_0 = 0.404$ and $\lambda = 1.57$. We note that this value for $\hat{\phi}_0$ is in good agreement with measured values of the porosity of unconsolidated very well sorted sands[6]. Figure 1 shows the values of β derived from these velocity and density data assuming a constant value of $\nu_m = 0.15$ along with this empirical function derived from them. The standard deviation of the fit is 0.004.

III. EXPERIMENTAL SUPPORT

Observations of brine-saturated sandstone density vs. P-wave velocity trends in deep water sediments from three different locations in the same geologic petroleum province (located roughly on a line separated by 25 km and 65 km) show two with anomalously low velocities at a given density with respect to the others (Fig. 2). The shales with which these anomalous sandstones are in contact, however, do not exhibit anomalous ρ vs. V_p trends. Notwithstanding their anomalous ρ vs. V_p relation , the relation of V_s to V_p in these anomalous sandstones as observed on wireline logs is not at all anomalous. Petrography of sand samples from these two locations shows a substantial fraction (~30%) of the rock solids to be lithic fragments the exact mineralogy and hence, the elastic properties of which are unknown. However, calculation using the current model and the average trend from many other wells assuming simple substitution of the lithic fragments for quartz grains in the rock matrix with no floating solid fraction (i.e., $f = 1.00$ and $f^* = 0.30$) and with both substantially more elastic and lighter minerals (i.e.. $R_K = K^*/K_g = 0.5$ and $R_\rho = \rho^*/\rho_g = 0.906$) and substantially less elastic and heavier minerals (i.e., $R_K = 2.0$ and $R_\rho = 1.057$) than quartz do not account for these anomalously slow rocks as shown in Fig. 3.

Calculation of the effects of removing some of the solid material from the load supporting matrix of the rock and allowing it to float suspended in the fluid filled pores without changing its elastic properties (i.e. with $R_K = 1.0 = R_\rho$), however, shows that only a small fraction of the solid matrix material, about 3% to 6% of the rock volume,

need be detached and made non load supporting to account for these anomalous trends (Fig. 4). This results from the substantial reduction in the matrix modulus, β, as the rock or matrix porosity increases.

A consequence of this model is that the anomalous sandstones have larger structural porosities than normal for a given fluid porosity and thus bulk density. As a result, the values of β for these anomalous rocks are lower than those for normal sandstones with the same density. Gassmann's equations, that is Eq. (2) and Eq. (3), predict that the effect of substitution of lighter and more compressible hydrocarbons for brine in a given fraction of the rock volume will produce a greater change in V_p than for a "normal" sandstone. Equation (2) to Eq. (4) and Eq. (6) allow one to compute the magnitude of this difference in the change of velocity. For the case studied here where $\phi_{flt} = 6\%$ and β is given by Eq. (6), the change in V_p for substitution of a typical oil for brine is 40% to 90% greater than would be obtained in a sandstone with $\phi_{flt} = 0\%$ with the same density characterized by the normal ρ vs. V_p trend.

Though it is not in general possible to give an algebraic expression for $\partial V_p / \partial \phi_{flt}\big|_{\phi}$ which does not involve f or f^*, in the case when the elastic properties of the second solid are the same as those of the first (i.e., for $R_\rho = 1 = R_K$) one finds

$$\left.\frac{\partial \rho}{\partial \phi_{flt}}\right|_{\phi} (\phi_{flt} = 0, \phi) = 0 \qquad (7)$$

and

$$\left.\frac{\partial V_p}{\partial \phi_{flt}}\right|_{\phi} (\phi_{flt}=0,\phi) = -\frac{\lambda\beta(\phi)}{2\hat{\phi}_0\left(1-\frac{\phi}{\hat{\phi}_0}\right)}\left[\frac{3(1-\nu_m)}{(1+\nu_m)} - F(2-F)\right]\frac{K_g}{\rho(\phi)V_p(\phi)}, \tag{8}$$

where

$$F = \frac{1-\beta(\phi)}{\left(\frac{K_g}{K_f}-1\right)\phi + 1 - \beta(\phi)} \tag{9}$$

and ν_m is assumed to be independent of $\hat{\phi}$. In the case of a sandstone matrix composed of quartz with $\nu_m = 0.15$ and the normal ρ vs. V_p trend shown for sandstones in the petroleum province shown above, $\partial V_p / \partial \phi_{flt}$ varies only from approximately $-11,600$ m/s at $\phi = 0.20$ to approximately $-9,600$ m/s at $\phi = 0.35$. This linear approximation thus results in a shift of the trend to the left in Fig. 4 with increasing ϕ_{flt} as observed.

The linearization in ϕ under the same conditions leading to Eqs. (7) and (8) produces

$$\left.\frac{\partial \rho}{\partial \phi}\right|_{\phi_{flt}} (\phi_{flt}=0,\phi) = -(\rho_g - \rho_f) \tag{10}$$

and

$$\left.\frac{\partial V_p}{\partial \phi}\right|_{\phi_{flt}} (\phi_{flt}=0,\phi) = (1+g)\left.\frac{\partial V_p}{\partial \phi_{flt}}\right|_{\phi} (\phi_{flt}=0,\phi), \tag{11}$$

where

$$g = \frac{2\left(\frac{K_g}{K_f} - 1\right)\left(\hat{\phi}_0 - \phi\right)F^2}{\lambda\beta(\phi)\left[\frac{3(1-\nu_m)}{(1+\nu_m)} - F(2-F)\right]}. \tag{12}$$

Again, for a normal sandstone as described above and with $\nu_m = 0.15$, g varies from approximately 0.21 at $\phi = 0.20$ to approximately 0.32 at $\phi = 0.35$.

Of course, any such model must also account for the absence of a significant difference in the V_s to V_p relation. It is easy to show (see the Appendix) that Eq. (1) to Eq. (3) along with Eq. (6) lead to the result that

$$V_p\left(\phi_{flt}, \phi\right) \cong V_p(0, \hat{\phi}) \tag{13}$$

and

$$V_s\left(\phi_{flt}, \phi\right) \cong V_s(0, \hat{\phi}) \tag{14}$$

at least for the case where $R_\rho = 1 = R_K$ and ν_m is independent of $\hat{\phi}$, which is surely a good approximation for $\phi_{flt} \ll \phi$. The approximation is valid for $K_g \gg K_f$ which is true for all sedimentary rocks and fluids. This means that in the current model, a change in ϕ_{flt} and thus in $\hat{\phi}$ without changing the fluid porosity ϕ does not significantly change the V_s to V_p relation. Instead a point on the curve describing this relation at $\phi_{flt} = 0$ merely moves to another point on this same curve at a lower value of V_p when $\phi_{flt} > 0$, so this model yields a result consistent with the observation that the V_s to V_p relation does not change (see Fig. 5).

An alternative model for these anomalous rocks which commonly occurs in nature is that they are composed of thinly laminated sands and shales with different

properties which cannot be detected as separate materials at the resolution of the logging devices. Calculations of the ρ vs. V_p relations using this model with values for the shale properties in contact with these sands at this location obtained from log measurements of much thicker shale units fail to reproduce the observed anomalous trends. An increase in the concentration of the shaels decreases V_p, but increases ρ to values greater than those observed in the log measurements. This model also predicts a shift in the V_s vs. V_p trend not seen in the data. The final piece of evidence that contradicts this model are independent core and log measurements that indicate that the rock is not thinly laminated.

This model requires floating grains in the pore spaces of the load supporting rock matrix at the anomalous locations which are not present in the rocks at the nearby locations where normal ρ vs. V_p relations are observed. Such floating solids are not easy to envision for a well sorted sandstone where all the grains have similar dimensions since the pore spaces in structures composed of such grains have similar sizes to the grains themselves so that no grain can readily fit in these pores without contacting several other grains and thus contributing to load support. On the other hand, for poorly sorted sandstones smaller grains of solid material would be available at the time of deposition when the rock matrix was constructed which could easily be trapped in the larger pores formed by contacts between multiple large grains and at least some of these may not have been fixed into the load supporting matrix by subsequent compaction. Consequently, one might expect a difference in the grain size distribution and sorting of the sandstones obtained from the anomalous and nearby normal locations.

Cores are available from both of the two anomalous locations as well as from a nearby location with a normal ρ vs. V_p trend. Grain size distributions were determined

on sandstone samples from these cores by laser grain size analysis[7], a standard petrophysical technique (see Fig. 6). We use as a measure of sorting the mean of the observed distribution of logarithmic grain diameters divided by its standard deviation. Figure 7 shows the mean ϕ_{flt} at each of these locations which best accounts for the ρ vs. V_p trend plotted against this sorting parameter.

IV. INFLUENCE ON FLUID FLOW

Sorting variations often correspond to variations in the relation between permeability and fluid porosity, ϕ, a crucial relation in determining the economic value of a hydrocarbon reservoir. Poorer sorting corresponds with lower permeability at a given ϕ. Logarithms of the measured permeabilities from several sandstone plugs obtained from cores at all three of the locations discussed above are plotted against their measured fluid porosities in Fig. 8a. Note the systematically higher permeabilities at the location with the normal ρ vs. V_p trend at a given porosity than at those locations with anomalous ρ vs. V_p trends. Using the mean ϕ_{flt} values determined above by fitting the ρ vs. V_p trends at each location in a regression of logarithmic permeability vs. porosity results in the plot shown in Fig. 8b. The uncertainty in the estimated logarithmic permeabilities is reduced by more than a factor of two with this regression,

$$\log(k) = 0.198\,\phi - 0.325\,\phi_{flt} - 1.76 \qquad (15)$$

where the permeability, k, is given in mD and both ϕ and ϕ_{flt} are expressed as percentages of rock volume. This suggests that permeability estimates and thus the economic viability of a potential reservoir may be substantially improved by observation

of the ρ vs. V_p trends which can be obtained from wireline logs without the need for permeability measurements on more than a few core samples. Note here that for the normal ρ vs. V_p trend with $\phi_{flt} = 0$, this regression corresponds to a permeability of 1 mD at $\phi = 8.9\%$ while for $\phi_{flt} = 5\%$, the same permeability requires $\phi = 17.1\%$ or $\hat{\phi} = 22.1\%$, a very substantial difference.

V. CAPTURE FRACTION OF GRAINS INTO MATRIX

One remaining facet of this model that completes the picture is the efficiency of capture of the smaller grains into the matrix. As a rock is formed with different grain sizes and then compacted with an effective stress, P_e (i.e., the difference between the externally applied stress and the pore pressure), we assume that a fraction of the smaller grains become part of the matrix, f_c, and others remain non load supporting (see Fig. 9). If this fraction is reasonably insensitive to the compaction, an assumption that is currently being numerically verified, the porosity may perhaps be modeled by an equation of the form

$$\phi = -\frac{\phi_{flt}}{1 - f_c} - A\left(1 - e^{-P_e / P_o}\right) + B, \tag{16}$$

where A, B and P_o are positive constants. When data from the three wells is regressed to determine the capture fraction, it is found to have a most likely value of 1/3 with a plus to minus two standard deviation range from 1/5 to 1/2. The most likely values for the constants are found to be $A = 0.88$, $B = 1.10$, and $P_o = 50$ bar. The uncertainties in these constants are highly correlated to the uncertainty in the capture ratio. This relationship is

critical in relating seismic reflectivity to permeability. One does not know, from reflectivity alone, the velocity vs. density trend and, therefore, ϕ_{flt}. But given knowledge of the effective stress, P_e, and Eq. (16), the dependence of Eq. (15) on ϕ_{flt} can be eliminated – permeability can then be estimated from seismic reflectivity.

VI. POSSIBLE CONFIRMING MEASURMENTS

It is not possible to directly observe which grains of the solids composing a sedimentary rock are load supporting and which are not using microscopic examination of thin sections, the standard tool for petrographic analysis, because these are essentially two dimensional samples so that not all the contacts of any particular grain with others can be observed. We, however, believe there are two possible experiments that can provide evidence for or against the proposed model. One may be able to determine quantitatively the amount of solids by volume participating in load support by forming an x-ray CAT scan image of a representative volume at suitable resolution and examining it carefully using 3D imaging techniques. Such images have been reported by investigators at the Australian National University[8]. In addition, we believe that spectra of the natural decay of vibrationally excited samples may well show broadening for samples containing "floating" solids compared with those for samples which do not. Rock matrices could also be numerically assembled, then examined for the amount of "floating" solids, and then simulated to determine their acoustic and flow properties. We are currently pursuing measurements of all three types.

VII. ACKNOWLEDGEMENTS

The authors would like to acknowledge the support of BHP Billiton Petroleum, and the help of Bruce Asher, Troy Thompson and Kai-Soon Tan.

REFERENCES

[1] F. Gassmann, Vierteljahrsschrift der Naturforschenden Gasellschaft in Zurich **96**, 1 (1951).

[2] M. Biot, J. Acoust. Soc. Amer. **28**, 168 (1956); M. Biot, J. Acoust. Soc. Amer. **28**, 179 (1956).

[3] A. Reuss and Z. Angew, Math. Mech. **9**, 49 (1929).

[4] W. Voight, *Lehrbuch der Kristallphysik* (Teubner, Leipzig, 1928).

[5] R. Hill, Proc. Phys. Soc. London Ser. A **65**, 349 (1952).

[6] D.C. Beard and P. Weyl, AAPG Bulletin **57**, 2 (1973).

[7] A. Name, Journal **00**, 111 (19xx).

[8] A. Sakellariou et al., Extended Abstracts of 73rd Annual Meeting of Society of Exploration Geophysicists, Dallas, paper RP2.6. SEG, Tulsa (2003).

APPENDIX: SHEAR VS. COMPRESSIONAL VELOCITY TRENDS

One has for V_p from Gassmann

$$V_p^2 = \frac{\hat{K}_g}{\hat{\rho}}\left[\frac{3(1-\nu_m)}{(1+\nu_m)}\beta + \frac{(1-\beta)^2}{\phi\left(\frac{\hat{K}_g}{\hat{K}_f}-1\right)+1-\beta}\right], \tag{A1}$$

where

$$\beta = \left(1-\frac{\hat{\phi}}{\phi_0}\right)^{\lambda}, \tag{A2}$$

and ϕ_0 is some constant. For $\rho^* = \rho_g$ and $K^* = K_g$ (i.e. for $R_\rho = 1 = R_K$) this gives

$$V_p^2(\phi_{flt},\phi) = \frac{K_g}{\rho}\left[\frac{3(1-\nu_m)}{(1+\nu_m)}\left(1-\frac{\hat{\phi}}{\phi_0}\right)^{\lambda} + \frac{\left[1-\left(\frac{\hat{\phi}}{\phi_0}\right)^{\lambda}\right]^2}{\hat{\phi}\left(\frac{K_g}{\hat{K}_f}-1\right)+1-\left(1-\frac{\hat{\phi}}{\phi_0}\right)^{\lambda}}\right], \tag{A3}$$

and for $\phi_{flt} = 0$,

$$V_p^2(0,\phi) = \frac{K_g}{\rho}\left[\frac{3(1-\nu_m)}{(1+\nu_m)}\left(1-\frac{\phi}{\phi_0}\right)^{\lambda} + \frac{\left[1-\left(\frac{\phi}{\phi_0}\right)^{\lambda}\right]^2}{\phi\left(\frac{K_g}{K_f}-1\right)+1-\left(1-\frac{\phi}{\phi_0}\right)^{\lambda}}\right], \tag{A4}$$

where

$$\hat{K}_f = \frac{\left(\phi + \phi_{flt}\right)}{\left(\phi + \frac{K_f}{K^*}\phi_{flt}\right)} K_f = \frac{K_f}{1 - \left(1 - \frac{K_f}{K^*}\right)\frac{\phi_{flt}}{\left(\phi + \phi_{flt}\right)}}. \tag{A5}$$

Now, for sedimentary rocks, $K_f \ll K^*$ since K_f is the bulk modulus of a fluid such as brine while K^* is the bulk modulus of a solid mineral such as silicon dioxide for a quartzitic sandstone, so we have

$$\hat{K}_f \cong \frac{K_f}{1 - \frac{\phi_{flt}}{\phi + \phi_{flt}}}, \tag{A6}$$

and since at least for small ϕ_{flt}, $\phi_{flt} \ll \phi + \phi_{flt}$, one has

$$K_f \cong \hat{K}_f, \tag{A7}$$

and thus,

$$V_p\left(\phi_{flt}, \phi\right) \cong V_p\left(0, \phi + \phi_{flt}\right). \tag{A8}$$

Now, one also has from Gassmann,

$$V_s^2\left(\phi_{flt}, \phi\right) = \frac{K_g}{\rho}\frac{3\left(1-2\nu_m\right)}{2\left(1+\nu_m\right)}\beta = \frac{K_g}{\rho}\frac{3\left(1-2\nu_m\right)}{2\left(1+\nu_m\right)}\left(1 - \frac{\hat{\phi}}{\phi_0}\right)^{\lambda}, \tag{A9}$$

whereas

$$V_s^2\left(0, \phi\right) = \frac{K_g}{\rho}\frac{3\left(1-2\nu_m\right)}{2\left(1+\nu_m\right)}\beta = \frac{K_g}{\rho}\frac{3\left(1-2\nu_m\right)}{2\left(1+\nu_m\right)}\left(1 - \frac{\phi}{\phi_0}\right)^{\lambda}. \tag{A10}$$

So,

$$V_s\left(\phi_{flt}, \phi\right) = V_s\left(0, \phi + \phi_{flt}\right). \tag{A11}$$

Hence, for this case (i.e., $R_\rho = 1 = R_K$), so long as $\phi_{flt} \ll \phi$ (i.e. for not too large values of ϕ_{flt}), the removal of some grains from the load-bearing matrix increasing the rock porosity and introducing them into the pore fluid approximately transforms one point on the V_s vs V_p curve to another point on that same curve.

FIGURE CAPTIONS

FIG. 1. Values of β derived from the typical sandstone ρ vs. V_p trends for sandstones in the petroleum province under study (circles) and the fit to them using Eq. (6) with $\lambda = 1.56$ and $\hat{\phi}_0 = 0.404$ (curve).

FIG. 2. Average sandstone ρ vs. V_p trend for the petroleum province under study (dashed line) and trends from three locations not widely separated (bold solid lines) one of which is consistent with the trend (I) and two of which are not (II and III). Error bars indicate two standard deviations of the fit to the ρ vs. V_p trends.

FIG. 3. ρ vs. V_p trend for typical sandstones in the petroleum province under study (dashed line) and for two anomalous locations (bold solid lines) with substantial amounts of lithic fragments. Calculations with both lighter and more elastic lithic fragments and heavier and stiffer lithic fragments in the rock matrix alone (solid lines) do not account for the anomalous trends. Error bars indicate two standard deviations of the fit.

FIG. 4. Sandstone ρ vs. V_p trends calculated with $R_K = 1 = R_\rho$ from the typical sandstone trend in the petroleum province under study for varying amounts of floating solids (solid lines) computed with this model overlaid on the observed trends of Fig. 2. Error bars indicate two standard deviations of the fit.

FIG. 5. Sandstone V_s vs. V_p trends calculated with $R_K = 1 = R_\rho$ from the typical sandstone trend (dashed line, petroleum province under study) for varying amounts of floating solids (solid lines) computed with this model overlaid on the observed trends seen at the wells. Error bars indicate two standard deviations of the fit. No significant differences are seen in any of these trends.

FIG. 6. Grain size distributions for the three wells that show a bimodal shape. Well I is plotted as the dashed line, well II as the solid line, and well III as the bold solid line.

FIG. 7. Floating solid fraction of rock volume derived from the observed ρ vs. V_p trends plotted against the sorting parameter (mean of the observed distribution of logarithmic grain diameters divided by its standard deviation). The solid line is linear fit to the points.

FIG. 8. (a) Log of the permeability measured on the core plotted vs. the porosity of the core. Shown for the three wells (black circles = well I, blue triangles = well II, red squares = well III), and linear fit curves to those points (black solid line = well I, blue dashed line = well II, red dotted line = well III). (b) Log of the permeability measured on

the core plotted vs. the permeability estimated by Eq. (15). Two standard deviation uncertainty in the regression is shown as the thin solid lines.

FIG. 9. (a) Picture of bimodal grain distribution before it is assembled and compacted. (b) the same grain distribution after it is assembled and compacted. The two small light grey grains are “floating”. The small dark grey grain is captured. The capture fraction is 1/3.

Figure 1.

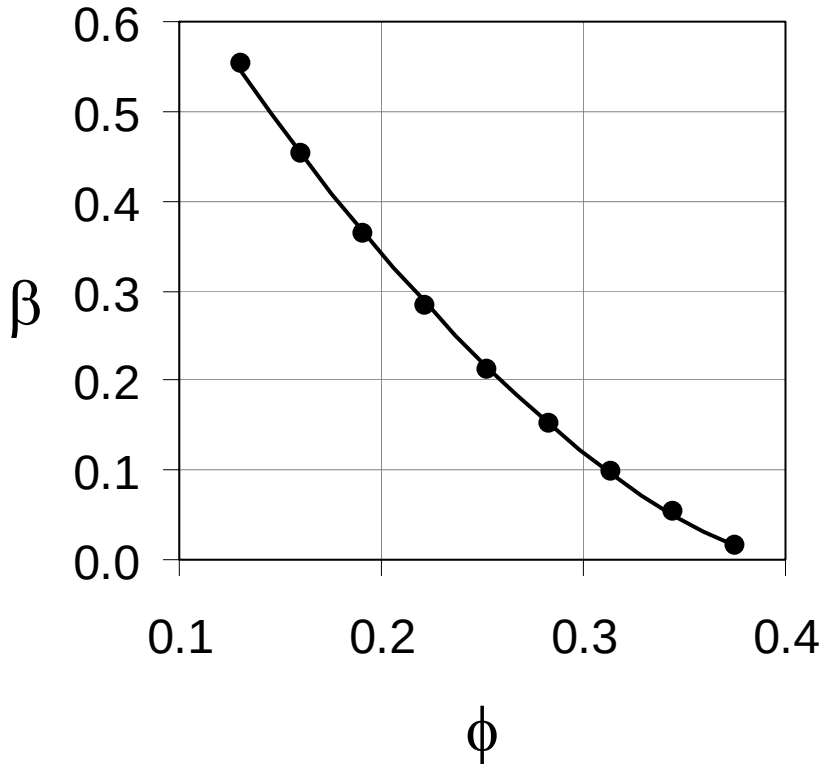

Figure 2.

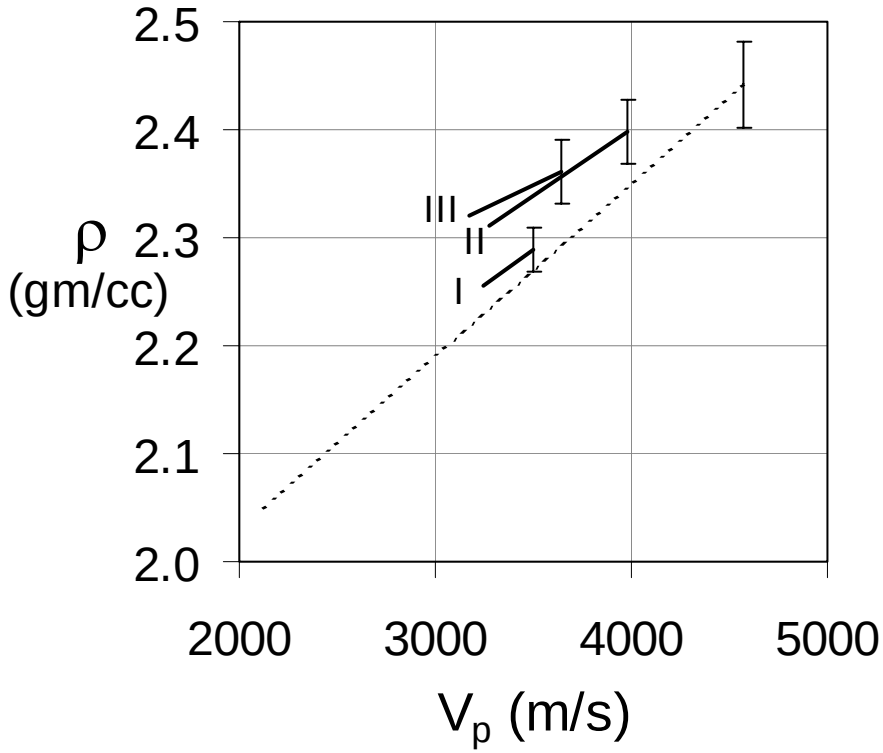

Figure 3.

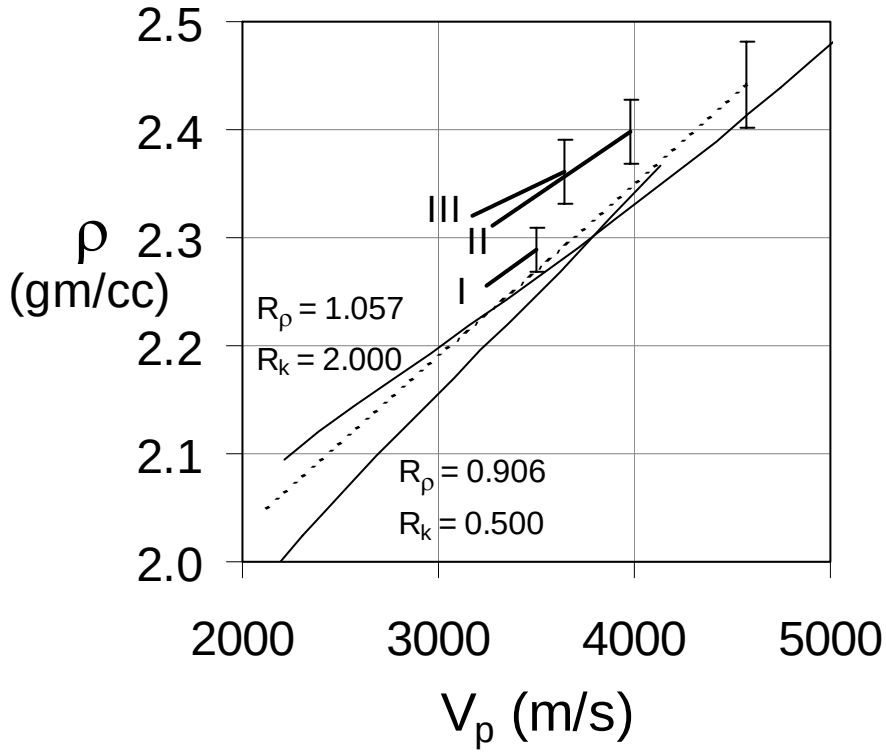
2.5
2.4
2.3
2.2
2.1
2.0
ρ (gm/cc)
III
II
I
R_ρ = 1.057
R_k = 2.000
R_ρ = 0.906
R_k = 0.500
2000
3000
4000
5000
V_p (m/s)

Figure 4.

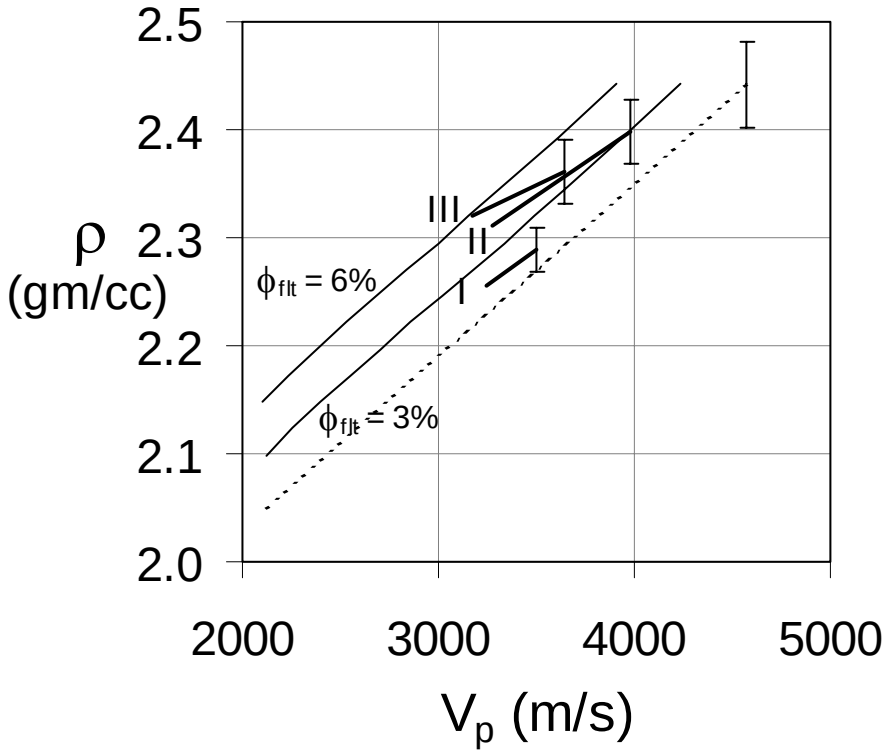
2.5
2.4
2.3
2.2
2.1
2.0
ρ (gm/cc)
III
II
I
ϕflt = 6%
ϕflt = 3%
2000
3000
4000
5000
Vp (m/s)

Figure 5.

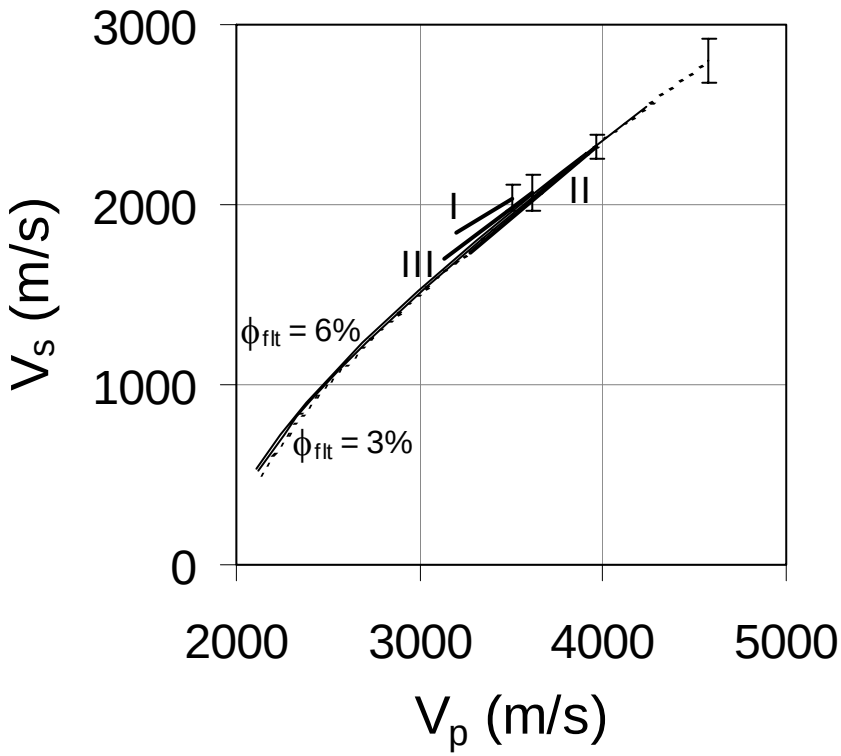
3000
2000
1000
0
2000
3000
4000
5000
V_s (m/s)
V_p (m/s)
I
II
III
ϕ_{flt} = 6%
ϕ_{flt} = 3%

Figure 6.

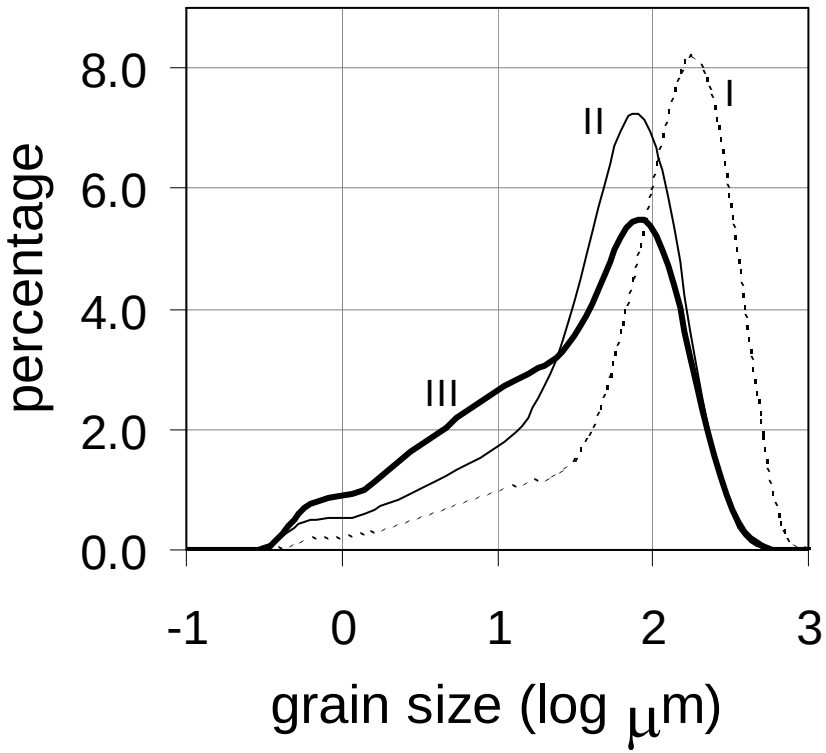

Figure 7.

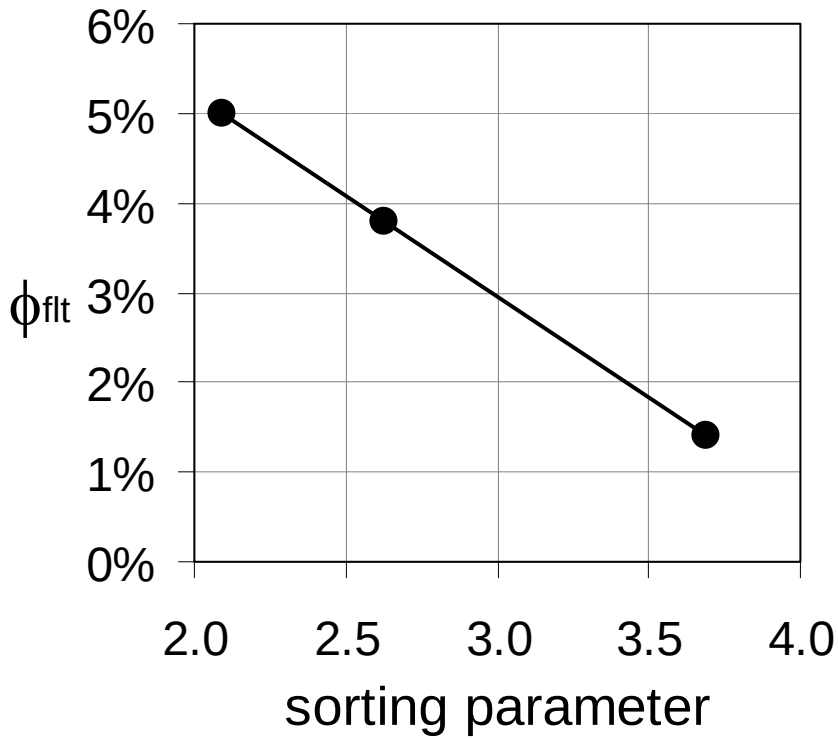

Figure 8.

(a)

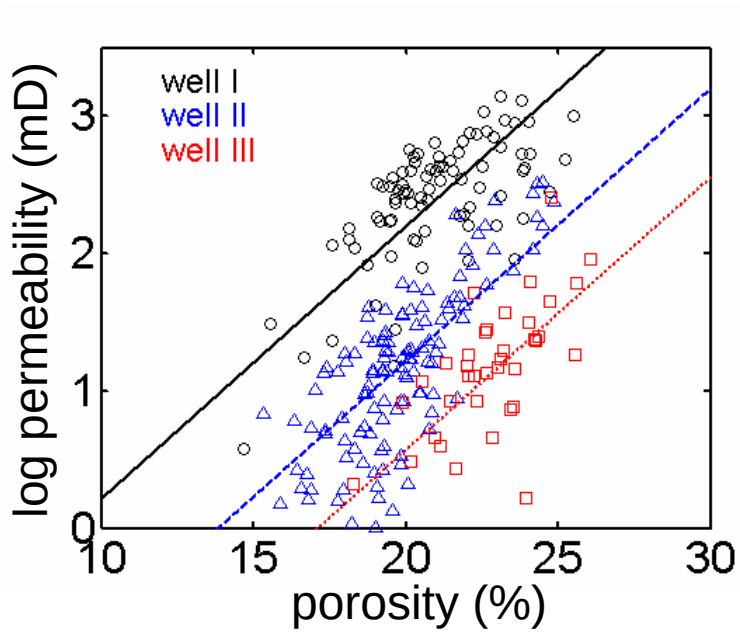
well I
well II
well III
log permeability (mD)
porosity (%)
0
1
2
3
10
15
20
25
30

(b)

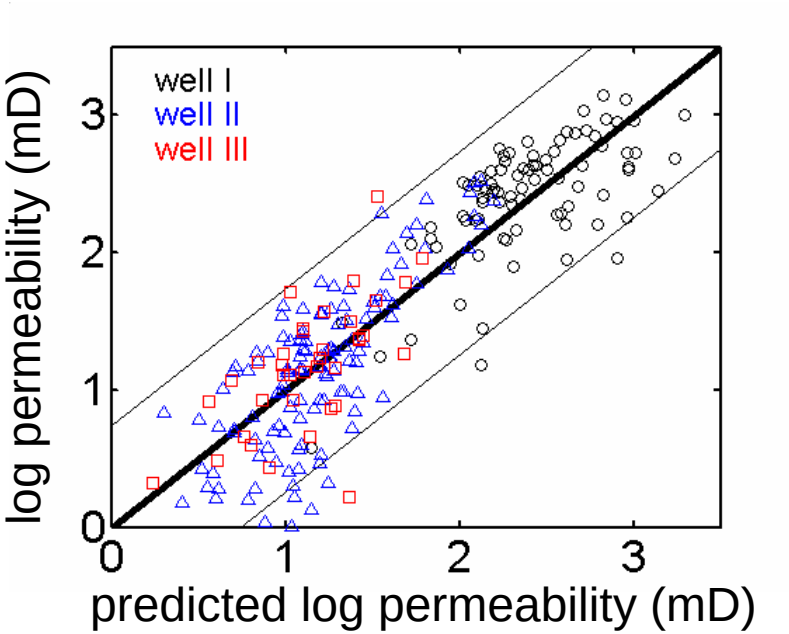
well I
well II
well III
log permeability (mD)
predicted log permeability (mD)
0
1
2
3

Figure 9.